

# Greybody factors of massive charged fermionic fields in a charged two-dimensional dilatonic black hole

Ramón Bécar<sup>1,a</sup>, P. A. González<sup>2,b</sup>, Joel Saavedra<sup>3,c</sup>, Yerko Vásquez<sup>4,d</sup>

<sup>1</sup> Departamento de Ciencias Matemáticas y Físicas, Universidad Católica de Temuco, Montt 56, Casilla 15-D, Temuco, Chile

<sup>2</sup> Facultad de Ingeniería, Universidad Diego Portales, Avenida Ejército Libertador 441, Casilla 298-V, Santiago, Chile

<sup>3</sup> Instituto de Física, Pontificia Universidad Católica de Valparaíso, Casilla 4950, Valparaíso, Chile

<sup>4</sup> Departamento de Física, Facultad de Ciencias, Universidad de La Serena, Avenida Cisternas 1200, La Serena, Chile

Received: 24 December 2014 / Accepted: 25 January 2015 / Published online: 6 February 2015

© The Author(s) 2015. This article is published with open access at Springerlink.com

**Abstract** We study massive charged fermionic perturbations in the background of a charged two-dimensional dilatonic black hole, and we solve the Dirac equation analytically. Then we compute the reflection and transmission coefficients and the absorption cross section for massive charged fermionic fields, and we show that the absorption cross section vanishes at the low- and high-frequency limits. However, there is a range of frequencies where the absorption cross section is not null. Furthermore, we study the effect of the mass and electric charge of the fermionic field over the absorption cross section.

## 1 Introduction

In order to find a clue on the Quantum Gravity problem in spacetime for which  $D = 4$ , a very rich model of different lower-dimensional gravity has been developed. In the particular case of  $D = 2$ , it is well known that the Einstein–Hilbert action has been used as the gravity sector. However, this model is locally trivial because the Einstein–Hilbert action in  $D = 2$  is just a topological invariant (Gauss–Bonnet theorem). If we want to obtain the dynamical degree of freedom, we need to couple this action with different fields besides the gravitational one. From this perspective, the dilatonic field has shown a very rich structure and includes black hole solutions. The dilatonic field naturally arises, for instance, in the compactifications from higher-dimensional gravity or from string theory. Two-dimensional dilatonic gravity has black hole solutions that play an important role and reveal various

physical aspects such as spacetime geometry, the quantization of gravity, and also physics related to string theory [1–3]. Furthermore, technical simplifications in two dimensions often lead to exact results, and it is hoped that this might help to address some of the conceptual problems posed by quantum gravity in higher dimensions. The exact solvability of two-dimensional models of gravity has been a useful tool for research in black hole thermodynamics [4–9]. Such lines of research are provided to give deeper understanding of some key issues, including the microscopic origin of the black hole entropy [10–12], and the final stages of black hole evaporation [13–15]. For a review of two-dimensional dilaton gravity [16], in the specific subject of black hole physics, there are several studies that have contributed to understanding the scattering and absorption properties of waves in black holes. Because the spacetime geometry surrounding a black hole is non-trivial, the Hawking radiation emitted at the event horizon is modified by this geometry, and therefore an asymptotic observer measuring the black hole thermal spectrum will measure a modified spectrum and no longer the well-known black body thermal spectrum [17]. The factors that modify the emitted spectrum of black holes are known as greybody factors and can be obtained through the classical scattering for fields under the influence of a black hole. Because Hawking radiation is of a quantum nature, the study of greybody factors allows increases of the semiclassical gravity dictionary, and also gives further steps into the quantum nature of black holes; for a review of this topic see [18].

In the present work we study the reflection and transmission coefficients, and the greybody factors of massive charged fermions fields on the background of two-dimensional charged dilatonic black holes [1, 19]. Greybody factors for scalar and fermionic field perturbations on the background of black holes have received much attention.

<sup>a</sup> e-mail: rbecar@uct.cl

<sup>b</sup> e-mail: pablo.gonzalez@udp.cl

<sup>c</sup> e-mail: joel.saavedra@ucv.cl

<sup>d</sup> e-mail: yvasquez@userena.cl

In this context, it was shown that for all spherically symmetric black holes, the low energy cross section for massless minimally coupled scalar fields is always the area of the horizon, where the contribution to the absorption cross section comes from the mode with lowest angular momentum [20–22]. However, for asymptotically AdS and Lifshitz black holes, it was observed that, at the low-frequency limit, there is a range of modes with highest angular momentum, which contribute to the absorption cross section in addition to the mode with lowest angular momentum [23–26]. Also, it was observed that the absorption cross section for the three-dimensional warped AdS black hole is larger than the area, even if the  $s$ -wave limit is considered [27]. Recently it has been found that the zero-angular-momentum greybody factors for non-minimally coupled scalar fields in four-dimensional Schwarzschild–de Sitter spacetime tends to zero around the zero-frequency limit [28]. Otherwise, for fermionic fields, it was shown that the absorption probability for bulk massive Dirac fermions in higher-dimensional Schwarzschild black hole increases with the dimensionality of the spacetime and decreases as the angular momentum increases. For this spacetime, it was also revealed that the absorption probability depended on the mass of the emitted field, that is, the absorption probability decreases or increases depending on the range of energy when the mass of the field increases. Also, it has been observed that the absorption probability increases for higher radii of the event horizon [29]; see for instance [30,31] for the decay of Dirac fields in higher-dimensional black holes. For further reference, massive charged scalar field perturbations of the Kerr–Newman black hole background were studied in [32,33], the absorption of photons and fermions by black holes in four-dimensions in [34], the fermion absorption cross section of a Schwarzschild black hole in [35], and charged fermionic perturbations in the Reissner–Nordstrom anti-de Sitter black hole background in [36]. For higher-dimensional black hole background see [37,38]. Furthermore, fermionic perturbations on the background of two-dimensional dilatonic black holes have been studied in which it was shown that the absorption cross section vanishes at the low- and high-frequency limits. However, there is a range of frequencies where the absorption cross section is not null [39]. Besides, charged fermionic field perturbations have been studied in order to obtain the quasinormal modes and to study the stability of these black holes [40].

This paper is organized as follows. In Sect. 2, we study massive charged fermionic perturbations in the background of two-dimensional dilatonic black holes, and in Sect. 3 we calculate the reflection and the transmission coefficients, and the absorption cross section. Finally, our conclusions are in Sect. 4.

## 2 Massive charged fermionic perturbations in two-dimensional charged dilatonic black holes

Let us begin with the effective action of Maxwell-gravity coupled to a dilatonic field  $\phi$  [3]:

$$S = \frac{1}{2\pi} \int d^2x \sqrt{-g} e^{-2\phi} \left( R - 4(\nabla\phi)^2 - \lambda - \frac{1}{4} F_{\mu\nu} F^{\mu\nu} \right), \quad (1)$$

where  $R$  is the Ricci scalar,  $\lambda$  is the central charge, and  $F_{\mu\nu}$  is the electromagnetic strength tensor. If we perform the variation of the metric, gauge, and dilaton field, we obtain the following equations of motions:

$$\begin{aligned} R_{\mu\nu} - 2\nabla_\mu \nabla_\nu \phi - \frac{1}{2} F_{\mu\sigma} F_\nu^\sigma &= 0, \\ \nabla_\nu (e^{-2\phi} F^{\mu\nu}) &= 0, \\ R - 4\nabla_\mu \nabla^\mu \phi + 4\nabla_\mu \phi \nabla^\mu \phi - \lambda - \frac{1}{4} F_{\mu\nu} F^{\mu\nu} &= 0. \end{aligned} \quad (2)$$

In order to describe the black hole solution, we considered the following form of the static metric for charged black holes:

$$ds^2 = -f(r) dt^2 + \frac{dr^2}{f(r)}, \quad (3)$$

in this expression,  $f(r) = 1 - 2me^{-Qr} + q^2 e^{-2Qr}$ ,  $\phi = \phi_0 - \frac{Q}{2}r$ , and  $F_{tr} = \sqrt{2}Qqe^{-Qr}$ . We used  $\lambda = -Q^2$  because of the asymptotic flatness condition for the spacetime required. It is well known that  $m$  and  $q$  (free parameters) are proportional to the black hole mass and charge, respectively. The positions of the horizons are given by

$$r_\pm = \frac{1}{Q} \ln(m \pm \sqrt{m^2 - q^2}), \quad (4)$$

we can obtain one single horizon solution ( $r_+$ ) if the following condition is fulfilled  $m^2 - q^2 \geq 0$ , from which it is straightforward to see that  $m^2 = q^2$  corresponds to an extremal case, where  $r_+ = r_-$ . On the other hand, using the coordinate transformation  $y = e^{-Qr}$  yields  $f(y) = 1 - 2my + q^2 y^2$ , where the spatial infinity is now located at  $y = 0$ . We can see that this solution represents the well-known string-theoretic black hole [1–3]. As is well known, charged fermionic perturbations on the background of two-dimensional charged dilatonic black hole are governed by the Dirac equation,

$$(\gamma^\mu (\nabla_\mu + iq' A_\mu) + m') \psi = 0, \quad (5)$$

where  $A_\mu$  denotes the electromagnetic potential,  $q'$  and  $m'$  denote the charge and the mass of the fermionic field  $\psi$ , respectively, and

$$\nabla_\mu = \partial_\mu + \frac{1}{2}\omega_{\mu}^{ab}J_{ab}, \tag{6}$$

represents the covariant derivative  $\nabla_\mu$ . In this last expression  $J_{ab} = \frac{1}{4}[\gamma_a, \gamma_b]$  are the generators of the Lorentz group, and  $\gamma^\mu$  are the gamma matrices in curved spacetime. These are defined by  $\gamma^\mu = e^\mu_a \gamma^a$ , where  $\gamma^a$  are the gamma matrices in flat spacetime. Here, we consider the following representation for the  $2 \times 2$  gamma matrices:

$$\gamma^0 = i\sigma^2, \quad \gamma^1 = \sigma^1, \tag{7}$$

where  $\sigma^i$  are the Pauli matrices. Now, in order to find the solution to the Dirac equation in this background we use the diagonal vielbein given by

$$e^0 = \sqrt{f(r)}dt, \quad e^1 = \frac{1}{\sqrt{f(r)}}dr, \tag{8}$$

and from the null torsion condition  $de^a + \omega^a_b \wedge e^b = 0$ , we obtain the spin connection

$$\omega^{01} = \frac{f'(r)}{2\sqrt{f(r)}}e^0. \tag{9}$$

Therefore, choosing the following ansatz for the fermionic field:

$$\psi = \frac{1}{f(r)^{1/4}}e^{-i\omega t} \begin{pmatrix} \psi_1 \\ \psi_2 \end{pmatrix}, \tag{10}$$

we obtain the following coupled system of equations:

$$\begin{aligned} \sqrt{f}\partial_r\psi_1 + \frac{i\omega}{\sqrt{f}}\psi_1 - \frac{\sqrt{2}iqq'}{\sqrt{f}}e^{-Qr}\psi_1 + m'\psi_2 &= 0 \\ \sqrt{f}\partial_r\psi_2 - \frac{i\omega}{\sqrt{f}}\psi_2 + \frac{\sqrt{2}iqq'}{\sqrt{f}}e^{-Qr}\psi_2 + m'\psi_1 &= 0. \end{aligned} \tag{11}$$

Now, decoupling the above equations we obtain the following equation for  $\psi_1$ :

$$\begin{aligned} 2f(r)^2\psi_1''(r) + f(r)f'(r)\psi_1'(r) \\ + e^{-2Qr}(4q^2q'^2 - 4\sqrt{2}e^{Qr}qq'\omega + 2e^{2Qr}\omega^2 \\ - 2e^{Qr}(m'^2e^{Qr} - \sqrt{2}iqq'Q)f(r) \\ - ie^{Qr}(-\sqrt{2}qq' + e^{Qr}\omega)f'(r))\psi_1(r) &= 0, \end{aligned} \tag{12}$$

and now performing the transformation  $y = e^{-Qr}$ , Eq. (12) becomes

$$\begin{aligned} \psi_1''(y) + \left(\frac{1}{y} + \frac{1/2}{y-y_+} + \frac{1/2}{y-y_-}\right)\psi_1'(y) \\ + \left(\frac{A_1}{y} + \frac{A_2}{y-y_+} + \frac{A_3}{y-y_-}\right) \\ \times \frac{1}{y(y-y_+)(y-y_-)}\psi_1(y) &= 0, \end{aligned} \tag{13}$$

where  $y_\pm$  are the roots of the function  $f(y) = 1 - 2my + q^2y^2$ , which are given by

$$y_\pm = \frac{m \mp \sqrt{m^2 - q^2}}{q^2}, \tag{14}$$

and the constants  $A_1$ ,  $A_2$ , and  $A_3$  are defined by the expressions

$$A_1 = \frac{1}{q^2Q^2}(\omega^2 - m'^2), \tag{15}$$

$$A_2 = y_+(y_+ - y_-) \left( \frac{1}{16} - \left( \frac{1}{4} - \frac{i\omega}{q^2Qy_+(y_+ - y_-)} + \frac{\sqrt{2}iq'}{qQ(y_+ - y_-)} \right)^2 \right), \tag{16}$$

$$A_3 = -y_-(y_+ - y_-) \left( \frac{1}{16} - \left( \frac{1}{4} + \frac{i\omega}{q^2Qy_-(y_+ - y_-)} - \frac{\sqrt{2}iq'}{qQ(y_+ - y_-)} \right)^2 \right). \tag{17}$$

Additionally, we perform the change of variable  $z = \frac{y_-}{y_+} \left( \frac{y-y_+}{y-y_-} \right)$ , and making the substitution

$$\psi_1(z) = z^\alpha(1-z)^\beta F(z), \tag{18}$$

in Eq. (13), we obtain the following equation for  $F(z)$ :

$$z(1-z)F''(z) + (c - (1+a+b)z)F'(z) - abF(z) = 0, \tag{19}$$

where

$$\alpha_\pm = \frac{1}{4} \pm \left( \frac{1}{4} - \frac{i\sqrt{2}q'}{Qq(y_- - y_+)} + \frac{i\omega y_-}{Q(y_- - y_+)} \right), \tag{20}$$

$$\beta_\pm = \pm \frac{i\sqrt{\omega^2 - m'^2}}{Q}. \tag{21}$$

Therefore, as Eq. (19) corresponds to the hypergeometric equation, its solution is given by

$$\begin{aligned} \psi_1 = C_1 z^\alpha(1-z)^\beta {}_2F_1(a, b, c, z) \\ + C_2 z^{1/2-\alpha}(1-z)^\beta {}_2F_1 \\ \times (a - c + 1, b - c + 1, 2 - c, z), \end{aligned} \tag{22}$$

which has three regular singular points at  $z = 0$ ,  $z = 1$ , and  $z = \infty$ . Here,  ${}_2F_1(a, b, c; z)$  denotes the Gauss hypergeometric function and  $C_1, C_2$  are integration constants and

$$a = \frac{1}{2} + 2\alpha + \beta + \frac{i\omega}{Q}, \tag{23}$$

$$b = \beta - \frac{i\omega}{Q}, \tag{24}$$

$$c = \frac{1}{2} + 2\alpha. \tag{25}$$

Now, imposing boundary conditions at the horizon, i.e., there are only ingoing waves, and choosing  $\alpha = \alpha_-$ , implies that  $C_2 = 0$ . Thus, the solution for  $\psi_1$  reduces to

$$\psi_1 = C_1 z^\alpha (1-z)^\beta {}_2F_1(a, b, c, z). \tag{26}$$

Otherwise, in order to find the solution for  $\psi_2$ , we use the change of variable defined before, i.e.,  $z = (\frac{y_-}{y_+})(\frac{y_- y_+}{y_- y_-})$ . Thus, the second equation of the system (11) can be written as

$$\begin{aligned} \psi_2'(z) - \frac{i\omega(y_- - y_+)}{(1-z)(y_- - y_+ z)Qf(z)}\psi_2 \\ + \frac{\sqrt{2}iqq'y_+y_-(y_- - y_+)}{(y_- - y_+ z)^2 Qf(z)}\psi_2 \\ + \frac{m'(y_- - y_+)}{(1-z)(y_- - y_+ z)\sqrt{f(z)}Q}\psi_1 = 0. \end{aligned} \tag{27}$$

Now, by using the integrating factor  $I$  given by

$$\begin{aligned} I = z^{-\frac{i}{2Q\sqrt{m^2-q^2}}(-\sqrt{2}qq'+(m+\sqrt{m^2-q^2})\omega)} (1-z)^{\frac{i\omega}{Q}} \\ = z^\alpha (1-z)^{\frac{i\omega}{Q}}, \end{aligned} \tag{28}$$

we integrate Eq. (27) and we obtain the solution

$$\begin{aligned} \psi_2 = -\frac{C_1 m'}{Q z^\alpha (1-z)^{\frac{i\omega}{Q}}} \int z'^{c-1} (1-z')^{a-c-1} {}_2F_1 \\ \times(a, b, c, z') dz', \end{aligned} \tag{29}$$

which can be written as

$$\psi_2 = -\frac{C_1 m' z^{\frac{1}{2}+\alpha} (1-z)^{\frac{i\sqrt{\omega^2-m'^2}}{Q}}}{Q(\frac{1}{2}+2\alpha)} {}_2F_1(a, b+1, c+1, z), \tag{30}$$

by using the relation

$$\begin{aligned} \int z^{c-1} (1-z)^{a-c-1} {}_2F_1(a, b, c, z) dz \\ = (1-z)^{a-c} z^c \frac{{}_2F_1(a, b+1, c+1, z)}{c}. \end{aligned} \tag{31}$$

### 3 Reflection coefficient, transmission coefficient, and absorption cross section

The reflection and transmission coefficients depend on the behavior of the radial function, at the horizon and at the asymptotic infinity, and they are defined by

$$\mathcal{R} := \left| \frac{\mathcal{F}_{\text{asympt}}^{\text{out}}}{\mathcal{F}_{\text{asympt}}^{\text{in}}} \right|; \quad \mathcal{T} := \left| \frac{\mathcal{F}_{\text{hor}}^{\text{in}}}{\mathcal{F}_{\text{asympt}}^{\text{in}}} \right|, \tag{32}$$

where  $\mathcal{F}$  is the flux, given by

$$\mathcal{F} = \sqrt{-g} \bar{\psi} \gamma^r \psi, \tag{33}$$

where  $\gamma^r = e_1^r \gamma^1$ ,  $\bar{\psi} = \psi^\dagger \gamma^0$ ,  $\sqrt{-g} = 1$ , and  $e_1^r = \sqrt{f(r)}$ , which yields

$$\mathcal{F} = |\psi_1|^2 - |\psi_2|^2. \tag{34}$$

The behavior of the fermionic field  $\psi$  at the horizon is given by Eq. (26) for  $\psi_1$  and Eq. (30) for  $\psi_2$  in the limit  $z \rightarrow 0$ . Then, using Eq. (34), we get the flux at the horizon,

$$\mathcal{F}_{\text{hor}}^{\text{in}} = |C_1|^2. \tag{35}$$

Besides, in order to obtain the asymptotic behavior of  $\psi_1$  and  $\psi_2$  we use the Kummer formula [41]:

$$\begin{aligned} {}_2F_1(a, b, c, z) = \frac{\Gamma(c)\Gamma(c-a-b)}{\Gamma(c-a)\Gamma(c-b)} {}_2F_1 \\ \times(a, b, a+b-c, 1-z) \\ + (1-z)^{c-a-b} \frac{\Gamma(c)\Gamma(a+b-c)}{\Gamma(a)\Gamma(b)} {}_2F_1 \\ \times(c-a, c-b, c-a-b+1, 1-z), \end{aligned}$$

in Eqs. (26) and (30), and by using Eq. (34) we obtain the flux at the asymptotic region  $z \rightarrow 1$ :

$$F_{\text{asympt}} = |A_1|^2 + |A_2|^2 - |B_1|^2 - |B_2|^2, \tag{36}$$

where

$$\begin{aligned} A_1 = C_1 \frac{\Gamma(c)\Gamma(c-a-b)}{\Gamma(c-a)\Gamma(c-b)}, \\ A_2 = C_1 \frac{\Gamma(c)\Gamma(a+b-c)}{\Gamma(a)\Gamma(b)}, \\ B_1 = -\frac{C_1 m'}{Q} \frac{\Gamma(c)\Gamma(c-a-b)}{\Gamma(c+1-a)\Gamma(c-b)}, \\ B_2 = -\frac{C_1 m'}{Q} \frac{\Gamma(c)\Gamma(a+b-c)}{\Gamma(a)\Gamma(b+1)}, \end{aligned}$$

where in the last two equations we have used the property  $\Gamma(c+1) = c\Gamma(c)$ . Therefore, the reflection and transmission coefficients are given by

$$\mathcal{R} = \frac{|B_1|^2 + |B_2|^2}{|A_1|^2 + |A_2|^2}, \tag{37}$$

$$\mathcal{T} = \frac{|C_1|^2}{|A_1|^2 + |A_2|^2}, \tag{38}$$

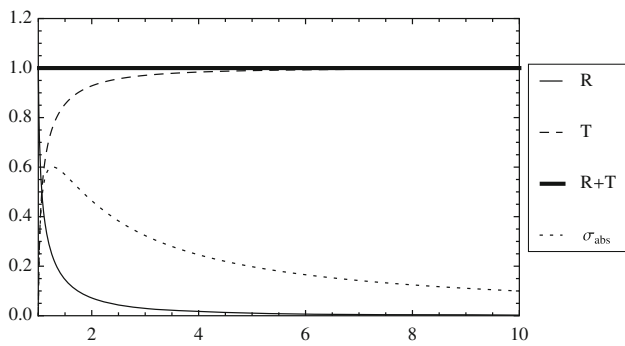


**Fig. 1** The reflection coefficient  $R$  (solid curve), the transmission coefficient  $T$  (dashed curve),  $R + T$  (thick curve), and the absorption cross section  $\sigma_{\text{abs}}$  (dotted curve) as a function of  $\omega$ , ( $1 \leq \omega$ ); for  $q = 0.5$ ,  $q' = 1$ ,  $m = 1$ ,  $m' = 1$ , and  $Q = 1$

and the absorption cross section,  $\sigma_{\text{abs}}$ , reads

$$\sigma_{\text{abs}} = \frac{1}{\omega} \frac{|C_1|^2}{|A_1|^2 + |A_2|^2}. \tag{39}$$

Now, we perform a numerical analysis of the reflection coefficient (37), transmission coefficient (38), and absorption cross section (39) of two-dimensional charged dilatonic black holes, for charged fermionic fields. In Fig. 1 we show the behavior of the reflection and transmission coefficients

and the absorption cross section, for charged fermionic fields for  $q = 0.5$ ,  $q' = 1$ ,  $m = 1$ ,  $m' = 1$ , and  $Q = 1$ . Essentially, we found that the reflection coefficient is 1 at the low-frequency limit, that is,  $\omega \approx m'$ , whereas for the high-frequency limit this coefficient is null, the opposite behavior of the transmission coefficient, with  $\mathcal{R} + \mathcal{T} = 1$ . Also, we observe that the absorption cross section is null at the low- and high-frequency limits, but there is a range of frequencies for which the absorption cross section is not null, and also it has a maximum value.

In addition, in Fig. 2 we show the behavior of the absorption cross section for different (positive and negative) values of  $q$ , where we observe that the absorption cross section is null at the low- and high-frequency limit, but there is a range of frequencies for which the absorption cross section is not null, and also it has a maximum value. Also, we observe in Figs. 2, 3, and 4 that for  $qq' > 0$  the absorption cross section decreases when  $qq'$  increases, due to the electric repulsion. However, for  $qq' < 0$  we found that the absorption cross section does not depend on the value of  $qq'$ . Also, we observe in Fig. 5 that the absorption cross section increases if the mass of the fermionic field increases; however, beyond a certain value of the frequency, the absorption cross section is constant and null for the high-frequency limit. On the other hand, in Fig. 6, we plot the absorption cross section for different

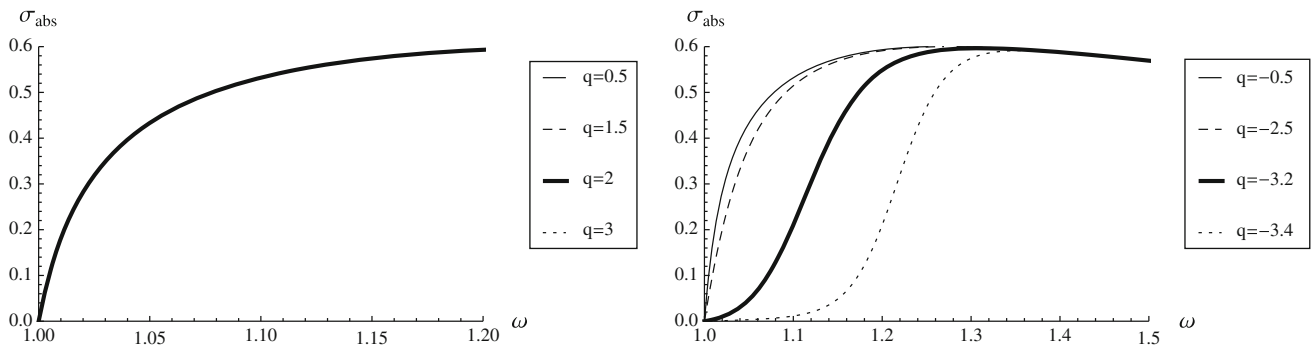


**Fig. 2** The absorption cross section  $\sigma_{\text{abs}}$  (dotted curve) as a function of  $\omega$ , ( $1 \leq \omega$ ); for  $q' = -1$ ,  $m = 3.5$ ,  $m' = 1$ ,  $Q = 1$ , and  $q = 0.5, 1.5, 2, 3$  for the left figure, and  $q = -0.5, -2.5, -3.2, -3.4$  for the right figure

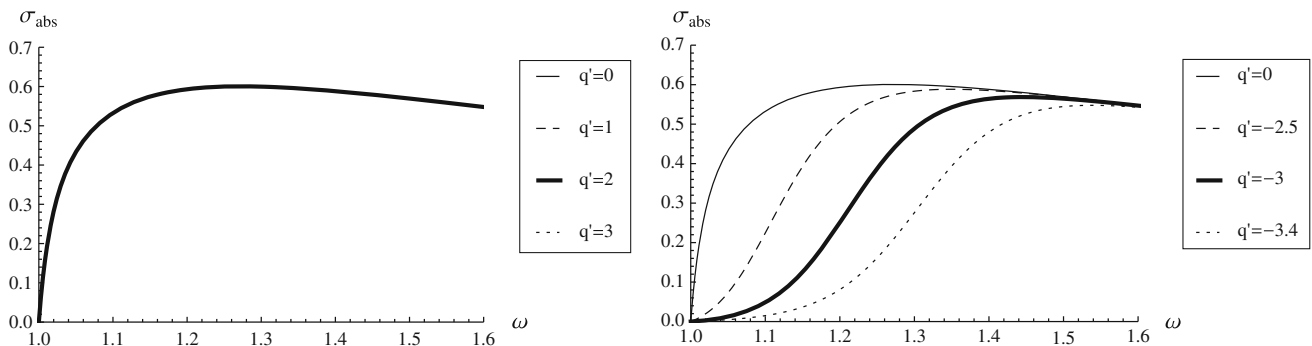


**Fig. 3** The absorption cross section  $\sigma_{\text{abs}}$  (dotted curve) as a function of  $\omega$ , ( $1 \leq \omega$ ); for  $m = 3.5$ ,  $m' = 1$ ,  $Q = 1$ ,  $q = -1.5$ , and  $q' = 0, 1, 2, 3$  for the left figure, and  $q' = 0, -2.5, -3, -3.4$  for the right figure

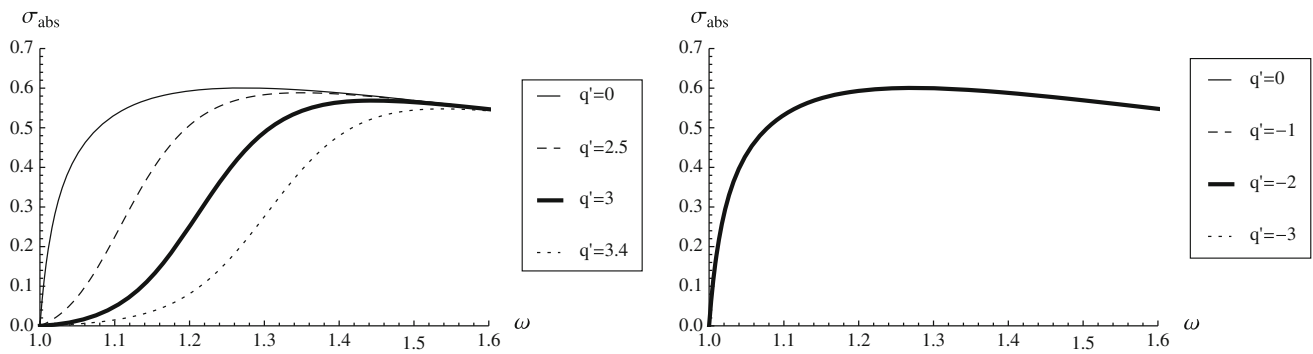


**Fig. 4** The absorption cross section  $\sigma_{\text{abs}}$  (dotted curve) as a function of  $\omega$ , ( $1 \leq \omega$ ); for  $q = 1.5$ ,  $m = 3.5$ ,  $m' = 1$ ,  $Q = 1$ , and  $q' = 0, 2.5, 3, 3.4$  for the left figure, and  $q' = 0, -1, -2, -3$  for the right figure

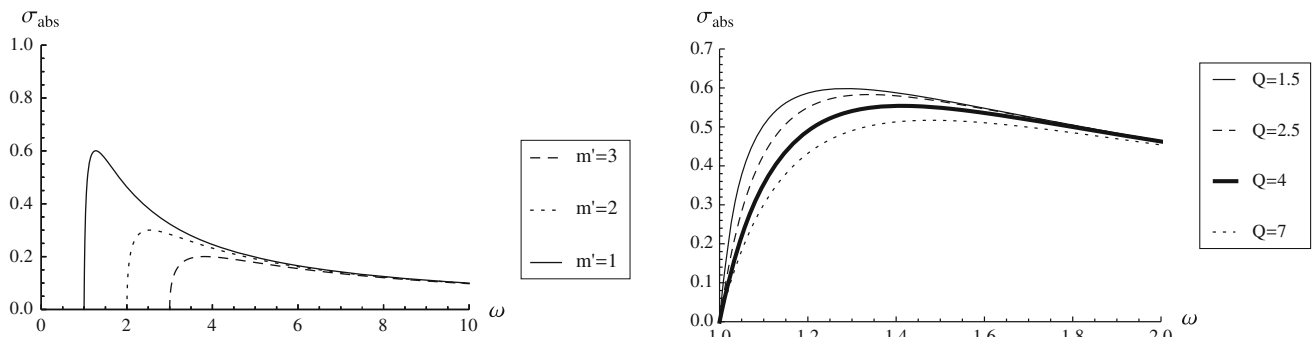


**Fig. 5** The absorption cross section  $\sigma_{\text{abs}}$  (dotted curve) as a function of  $\omega$ ; for  $q = 0.5$ ,  $q' = 1$ ,  $m = 1$ ,  $Q = 1$ , and  $m' = 1, 2, 3$

**Fig. 7** The absorption cross section  $\sigma_{\text{abs}}$  (dotted curve) as a function of  $\omega$ , ( $1 \leq \omega$ ); for  $q = 0.5$ ,  $q' = 1$ ,  $m = 1$ ,  $m' = 1$ , and  $Q = 1.5, 2.5, 4, 7$

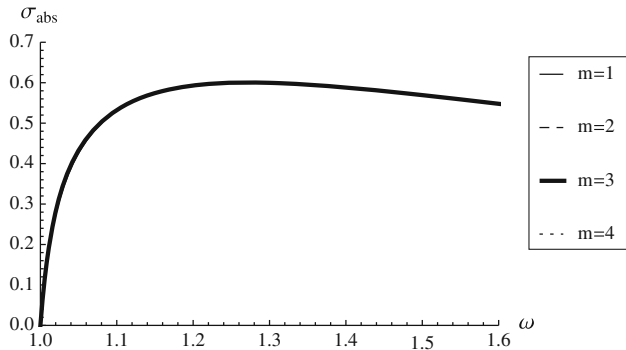


**Fig. 6** The absorption cross section  $\sigma_{\text{abs}}$  (dotted curve) as a function of  $\omega$ ; for  $q = 0.5$ ,  $q' = 1$ ,  $m' = 1$ ,  $Q = 1$ , and  $m = 1, 2, 3, 4$

values of  $m$  and we observe that it does not depend on the mass of the black hole. Finally, we observe that the absorption cross section increases if  $Q$  decreases; see Fig. 7.

### 4 Conclusions

In this work we have studied massive charged fermionic perturbations on the background of two-dimensional charged dilatonic black holes, and we have computed the reflection and transmission coefficients, and the absorption cross sec-

tion, and we have shown numerically that the absorption cross section vanishes at the low- and high-frequency limits. Therefore, a wave emitted from the horizon, with low or high frequency, does not reach infinity and is totally reflected, since the fraction of particles penetrating the potential barrier vanishes; however, we have shown that there is a range of frequencies where the absorption cross section is not null. The reflection coefficient is 1 at the low-frequency limit and null for the high-frequency limit, demonstrating a behavior opposite to the transmission coefficient, with  $\mathcal{R} + \mathcal{T} = 1$ . It is worth mentioning that these results, greybody factors, are consistent with other geometries of dilatonic black holes [39,42,43]. Also, we have studied the effect of the electric charge of the fermionic field over the absorption cross section, and we have observed different behaviors depending on the sign and the value of the product of the charges  $\propto qq'$ . That is, for  $qq' > 0$  we have found that the absorption cross section decreases when  $qq'$  increases, due to the electric repulsion. However, for  $qq' < 0$  we have found that the absorption cross section does not depend on the value of  $qq'$ , and for this case we obtain the same value of the absorption cross section as for the case  $q' = 0$ . Also, we have found that the absorption cross section increases if the mass of the

fermionic field increases; however, beyond a certain value of the frequency, the absorption cross section is constant. Also, we have found that the absorption cross section for massive charged fermionic fields in a charged two-dimensional dilatonic black hole does not depend on the mass of the black hole.

**Acknowledgments** This work was funded by Comisión Nacional de Ciencias y Tecnología through FONDECYT Grants 11140674 (PAG), 1110076 (JS) and 11121148 (YV) and by DI-PUCV Grant 123713 (JS). R. B. acknowledges the hospitality of the Universidad Diego Portales where part of this work was undertaken.

**Open Access** This article is distributed under the terms of the Creative Commons Attribution License which permits any use, distribution, and reproduction in any medium, provided the original author(s) and the source are credited.  
Funded by SCOAP<sup>3</sup> / License Version CC BY 4.0.

## References

1. E. Witten, Phys. Rev. D **44**, 314 (1991)
2. E. Teo, Phys. Lett. B **430**, 57 (1998)
3. M.D. McGuigan, C.R. Nappi, S.A. Yost, Nucl. Phys. B **375**, 421 (1992)
4. J.P.S. Lemos, Phys. Rev. D **54**, 6206 (1996). [arXiv:gr-qc/9608016](#)
5. D. Youm, Phys. Rev. D **61**, 044013 (2000). [arXiv:hep-th/9910244](#)
6. J.L. Davis, L.A. Pando Zayas, D. Vaman, JHEP **0403**, 007 (2004). [arXiv:hep-th/0402152](#)
7. D. Grumiller, R. McNees, JHEP **0704**, 074 (2007). [arXiv:hep-th/0703230](#) [HEP-TH]
8. H. Quevedo, A. Sanchez, Phys. Rev. D **79**, 087504 (2009). [arXiv:0902.4488](#) [gr-qc]
9. A. Belhaj, M. Chabab, H. El Moumni, M.B. Sedra, A. Segui, Int. J. Geom. Meth. Mod. Phys. **11**(5), 1450047 (2014). [arXiv:1311.2801](#) [hep-th]
10. R.C. Myers, Phys. Rev. D **50**, 6412 (1994). [arXiv:hep-th/9405162](#)
11. J. Sadeghi, M.R. Setare, B. Pourhassan, Acta Phys. Pol. B **40**, 251 (2009). [arXiv:0707.0420](#) [hep-th]
12. S. Hyun, W. Kim, J.J. Oh, E.J. Son, JHEP **0704**, 057 (2007). [arXiv:hep-th/0702170](#)
13. W.T. Kim, J.J. Oh, J.H. Park, Phys. Rev. D **60**, 047501 (1999). [arXiv:hep-th/9902093](#)
14. E.C. Vagenas, Mod. Phys. Lett. A **17**, 609 (2002). [arXiv:hep-th/0108147](#)
15. D.A. Easson, JHEP **0302**, 037 (2003). [arXiv:hep-th/0210016](#)
16. D. Grumiller, W. Kummer, D.V. Vassilevich, Phys. Rep. **369**, 327 (2002). [arXiv:hep-th/0204253](#)
17. J.M. Maldacena, A. Strominger, Phys. Rev. D **55**, 861 (1997). [arXiv:hep-th/9609026](#)
18. T. Harmark, J. Natario, R. Schiappa, Adv. Theor. Math. Phys. **14**, 727 (2010). [arXiv:0708.0017](#) [hep-th]
19. V.P. Frolov, A. Zelnikov, Phys. Rev. D **63**, 125026 (2001). [arXiv:hep-th/0012252](#)
20. A.A. Starobinsky, Sov. Phys. JETP **37**, 28 (1973)
21. A.A. Starobinsky, S.M. Churilov, Sov. Phys. JETP **38**, 1 (1974)
22. S.R. Das, G.W. Gibbons, S.D. Mathur, Phys. Rev. Lett. **78**, 417 (1997)
23. C. Campuzano, P. Gonzalez, E. Rojas, J. Saavedra, JHEP **1006**, 103 (2010)
24. P. Gonzalez, E. Papantonopoulos, J. Saavedra, JHEP **1008**, 050 (2010)
25. P.A. Gonzalez, J. Saavedra, Int. J. Mod. Phys. A **26**, 3997 (2011)
26. P.A. Gonzalez, F. Moncada, Y. Vasquez, Eur. Phys. J. C **72**, 2255 (2012)
27. J.J. Oh, W. Kim, Eur. Phys. J. C **65**, 275 (2010)
28. L.C.B. Crispino, A. Higuchi, E.S. Oliveira, J.V. Rocha, Phys. Rev. D **87**, 10, 104034 (2013). [arXiv:1304.0467](#) [gr-qc]
29. M. Rogatko, A. Szyplowska, Phys. Rev. D **79**, 104005 (2009). [arXiv:0904.4544](#) [hep-th]
30. R. Moderski, M. Rogatko, Phys. Rev. D **77**, 124007 (2008). [arXiv:0805.0665](#) [hep-th]
31. G.W. Gibbons, M. Rogatko, A. Szyplowska, Phys. Rev. D **77**, 064024 (2008). [arXiv:0802.3259](#) [hep-th]
32. R.A. Konoplya, A. Zhidenko, Phys. Rev. D **88**, 024054 (2013). [arXiv:1307.1812](#) [gr-qc]
33. R.A. Konoplya, A. Zhidenko, Phys. Rev. D **89**, 8, 084015 (2014). [arXiv:1402.1998](#) [gr-qc]
34. S.S. Gubser, Phys. Rev. D **56**, 7854 (1997). [arXiv:hep-th/9706100](#)
35. C. Doran, A. Lasenby, S. Dolan, I. Hinder, Phys. Rev. D **71**, 124020 (2005). [arXiv:gr-qc/0503019](#)
36. R.G. Cai, Z.Y. Nie, B. Wang, H.Q. Zhang. [arXiv:1005.1233](#) [gr-qc]
37. E. Jung, S. Kim, D.K. Park, JHEP **0409**, 005 (2004). [arXiv:hep-th/0406117](#)
38. E. Jung, S. Kim, D.K. Park, Phys. Lett. B **614**, 78 (2005). [arXiv:hep-th/0503027](#)
39. R. Becar, P.A. Gonzalez, Y. Vasquez, Eur. Phys. J. C **74**, 8, 3028 (2014). [arXiv:1404.6023](#) [gr-qc]
40. R. Becar, P.A. Gonzalez, Y. Vasquez, Eur. Phys. J. C **74**, 2940 (2014). [arXiv:1405.1509](#) [gr-qc]
41. M. Abramowitz, A. Stegun, *Handbook of Mathematical functions* (Dover publications, New York, 1970)
42. J.Y. Kim, H.W. Lee, Y.S. Myung, Mod. Phys. Lett. A **10**, 2853 (1995). [arXiv:hep-th/9510124](#)
43. J. Abedi, H. Arfaei. [arXiv:1308.1877](#) [hep-th]